

Article

Synergistic Effect of Micro-Silica and Recycled Tyre Steel Fiber on the Properties of High-Performance Recycled Aggregate Concrete

Muhammad Talha Amir^{1,2}, Sobia Riaz³, Hawreen Ahmed^{4,5,*}, Syed Safdar Raza^{3,*}, Ahmed Ali A. Shohan⁶ 
and Saleh Alsulamy⁶

- ¹ Department of Civil Engineering, University of Engineering and Technology, Taxila 47050, Pakistan; ascepak@gmail.com
- ² House of Property and Entrepreneurship (HOPE), Wallayat Complex, Plaza 74, Phase 7 Bahria Town, Islamabad 46000, Pakistan
- ³ Department of Civil Engineering, Faculty of Engineering, Bahauddin Zakariya University, Multan 66000, Pakistan; sobiariaz@bzu.edu.pk
- ⁴ Department of Highway and Bridge Engineering, Technical Engineering College, Erbil Polytechnic University, Erbil 44001, Iraq
- ⁵ Department of Civil Engineering, College of Engineering, Nawroz University, Duhok 42001, Iraq
- ⁶ Architecture & Planning Department, College of Engineering, King Khalid University (KKU), Abha 61411, Saudi Arabia; ashohan@kku.edu.sa (A.A.A.S.)
- * Correspondence: hawreen.a@gmail.com (H.A.); safdarshah91@bzu.edu.pk (S.S.R.)

Abstract: The present research investigates the mechanical and physical properties of recycled aggregate concrete (RAC) modified with micro-silica (MS) and recycled tire steel fiber (RTSF). Natural coarse aggregates (NCA) were completely replaced by recycled coarse aggregates (RCA) to prepare RAC. High-strength RAC mixes were prepared by replacing 5% and 10% of Portland cement with MS. With each level of MS, RTSF was incorporated as 0%, 0.5%, 1 and 2% by volume fraction. In addition to mechanical properties, ultrasonic pulse velocity (UPV), electrical resistivity (ER), and water absorption (WA) of the mixes were also evaluated. The performance of modified RAC mixtures was also compared with plain natural aggregate concrete (PNAC). The experimental investigation revealed that RTSF substantially increased the tensile strength of RAC, whereas MS improved the durability of RTSF-reinforced RAC. RAC made with 1% RTSF and 10% MS showed 54% more splitting-tensile strength compared to the PNAC. The WA capacity of RAC incorporating 10% MS was 15–22% lower than that of the PNAC.

Keywords: waste tyres; construction waste; water absorption; supplementary binder; steel fiber; optimization; fibers and environment



check for updates

Citation: Amir, M.T.; Riaz, S.; Ahmed, H.; Raza, S.S.; Shohan, A.A.A.; Alsulamy, S. Synergistic Effect of Micro-Silica and Recycled Tyre Steel Fiber on the Properties of High-Performance Recycled Aggregate Concrete. *Sustainability* **2023**, *15*, 8642. <https://doi.org/10.3390/su15118642>

Academic Editor: José Ignacio Alvarez

Received: 26 March 2023

Revised: 11 May 2023

Accepted: 22 May 2023

Published: 26 May 2023



Copyright: © 2023 by the authors. Licensee MDPI, Basel, Switzerland. This article is an open access article distributed under the terms and conditions of the Creative Commons Attribution (CC BY) license (<https://creativecommons.org/licenses/by/4.0/>).

1. Introduction

Many countries are suffering a scarcity of space to landfill construction and demolition (C&D) wastes. Uncontrolled urbanization has caused a massive boom in the construction industry. The state-of-the-art structures are replacing the insufficient and older ones and consequently, it led to the increased generation of C&D wastes. Due to the scarcity of landfilling space in urban regions, C&D waste is normally dumped along with domestic waste which causes severe environmental and social issues. Globally, around 40 major countries produce more than 3 billion metric tons of C&D waste per year [1]. The most effective method to deal with a massive quantity of C&D waste is to recycle it as construction aggregate and use them in the construction of buildings and roads [2]. Reusing C&D waste as construction aggregate is a win-win model to save both environment and humans from the adverse impacts of the construction industry.

In the past decade, researchers advanced their interest in appraising the performance of structural concrete produced with recycled coarse aggregates (RCA). Successful applications of RCA have been reported in rigid concrete pavements and building structures [3,4]. Hoffman et al. [5] (2012) assessed the performance of reinforced concrete (RC) elements with RCA. They reported that RC beams made with RCA show insignificant changes in shear strength compared to those made with natural coarse aggregates (NCA). The life cycle assessment studies have confirmed the environmental benefits of RCA application in structural concrete [2,6]. Not only recycled aggregate concrete (RAC) has a lower CO₂ footprint than conventional plain natural aggregate concrete (PNAC) [7], but it also helps in avoiding the potential increase in toxicity of soils due to uncontrolled disposal of C&D wastes [6,8,9].

Due to the existence of adhered mortar, RCA is weaker than NCA. Therefore, RAC has inferior properties compared to natural aggregate concrete (NAC) for the same volume of aggregate. To address the drawbacks of RAC, researchers have preferred using additional cementitious materials like silica fume/micro-silica, metakaolin, slag, fly ash, etc. [10–13] and fiber reinforcements (i.e., glass, steel, macro-synthetic fibers, etc.) [14–17]. SCMs are highly useful in enhancing the durability characteristics of RAC such as imperviousness against harmful fluids [14,18], acid attack resistance [14,19], chloride-ion permeability resistance [11,19], etc. High-performance admixtures like silica fume or micro-silica (MS) have shown positive effects on the strength enhancement of RAC, in addition to its phenomenal contribution to durability [11,20–22].

Fiber reinforcement overcomes the inherent brittleness of plain concrete. It is an excellent option to advance the tensile and flexural strength of RAC [23,24]. The effect of several types of fibers i.e., steel, glass, polypropylene, hybrid fibers, etc. have been studied on the performance of RAC [14,16,25–27]. Generally, fiber-reinforcement significantly enhanced the tensile ductility, shrinkage and abrasion resistance and impact toughness of concrete [28–30]. It has shown a positive role in some durability aspects, such as control over the degradation and abrasion of plain concrete surfaces [31,32]. The acid-attack durability of plain RAC has been reported to improve due to the addition of steel and glass fibers [14,33]. Therefore, the use of fibers can increase the life of a structure and minimize the maintenance cost.

Despite numerous benefits, especially in terms of improved ductility behavior and toughness, artificial fibers are expensive and possess a high CO₂ footprint compared to the SCMs and conventional constituents of concrete. For instance, artificial steel fiber (ASF) at a 1% volume fraction can increase the cost of concrete by twice, as shown by literature [34,35]. The carbon footprint of plain concrete increased by more than 50% at 1% volume of ASF [34,36]. Therefore, ASF, despite its phenomenal utilization ratio in tensile ductility [25], is an expensive option to upgrade the performance of RAC. Other than artificial fibers, cheap alternatives for fiber-reinforcements are recycled tyre steel fibers (RTSF) [37–39] and organic fibers [40,41] which are currently being examined for their effects on the mechanical and durability properties of concrete.

RTSF is recovered from the steel bead wires of scrap tyres, and it possesses high tensile strength and toughness comparable to ASF since new tyres are manufactured with high-grade tension steel wires [42]. The flexural behavior, residual strength and energy absorption capacity of RTSF-reinforced concrete and ASF-reinforced concrete is almost similar [39,43]. Hence, RTSF is a suitable, eco-friendly, and low-cost fiber reinforcement. Until now, very few studies [44,45] have appraised the performance of RAC incorporating RTSF. Existing studies showed [44,45] that using 0.5–1% volume RTSF notably increased the splitting-tensile strength (f_{ctm}) and flexural strength of RAC, while it showed a marginal effect on the compressive strength (f_{cm}).

The coupling effects of MS and RTSF on the performance of RAC have never been studied. Since modern structures require high strength, excellent durability, and ductility behavior, therefore, the performance of RAC must be studied with the combined incorporation of MS and RTSF. The durability and ductility benefits of SCMs and fiber, respectively can be combined by the simultaneous addition of MS and RTSF in RAC. Eventually, it

would lead to the development of low-cost and sustainable high-performance RAC. Therefore, the present study is devoted to examining the mechanical and physical properties of RAC with different levels of MS (0, 5, and 10%) and RTSF (0, 0.5, 1, and 2%). Mechanical properties included f_{cm} (7, 28, 90, and 180 days) and f_{ctm} (28 and 90 days). Physical properties included ER, WA, and UPV were assessed at the age 28 and 90 days. Statistical correlations between mechanical and physical parameters were analysed.

2. Materials and Methods

2.1. Materials

2.1.1. Cement and Micro-Silica

Portland cement of '53 Grade' was utilized as the main binder to prepare all concrete mixes. The properties of Portland cement complied with ASTM C150 [46]. The properties of cement are given in Table 1. Commercially available high-performance MS was used as a partial replacement for cement. It has a silica oxide (SiO_2) content of approx. 98.5%. The specific gravity (G_s) and specific surface area of MS particles were 2.18 and 27,000 m^2/kg , respectively. These properties of MS came with technical datasheet. The particle size distribution of cement and MS samples is illustrated in Figure 1.

Table 1. Chemical, physical and mechanical properties of cement.

Chemical Properties	% Composition
Lime (CaO)	63.15
Alumina (Al_2O_3)	5.24
Silica (SiO_2)	19.6
Iron Oxide (Fe_2O_3)	4.36
Magnesia (MgO)	0.76
Loss in the ignition (LOI)	1.13
Physical Properties	Result
Specific gravity	3.11
Specific surface area (m^2/kg)	371
Initial setting time (h)	1.45
Final setting time (h)	2.93
7-days f_{cm}	45.5
28-days f_{cm}	52.4

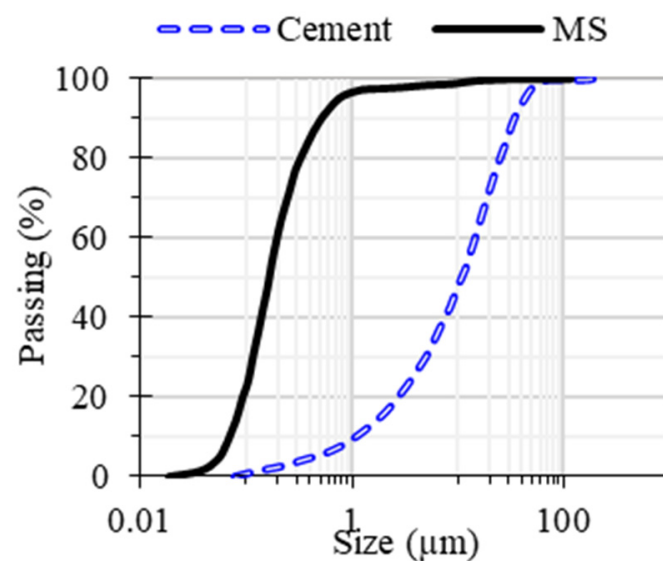


Figure 1. Gradation of binding materials.

2.1.2. Aggregates

For fine aggregates, siliceous sand from ‘The Lawrancepur’ quarry was used. This sand is used for the production of high-strength concrete in Pakistan. For NCA, crushed dolomitic sandstone of Kirana-Hills was used to prepare PNAC. The maximum aggregate size was 12.5 mm for NCA. The general properties of aggregates are given in Table 2. For the gradation of aggregates, ASTM C33 [47] was followed. For the determination of specific gravity (Gs) and WA, ASTM C127 [48] and ASTM C128 [49] were adopted for coarse aggregates and fine aggregates, respectively.

Table 2. Characteristics of aggregate samples.

Aggregate Type	Grain Size (mm)		24-h' WA (%)	Gs	FM
	Max.	Min.			
Sand	4.75	0.075	0.81	2.68	2.91
Crushed sandstone	12.5	2.36	0.93	2.73	-
RCA (Crushed-concrete waste)	12.5	2.36	3.56	2.57	-

RCA was derived from old high-strength concrete samples aged approx. 2 years. The aged samples were manually crushed to prepare. The samples were crushed and graded according to the size of NCA. The absorption capacity of RCA is almost four times higher than that of the NCA. Therefore, RCA was used in saturated surface dried (SSD) conditions to prepare concrete mixes. The properties of RCA are given in Table 1. Gradation charts of aggregates are shown in Figure 2.

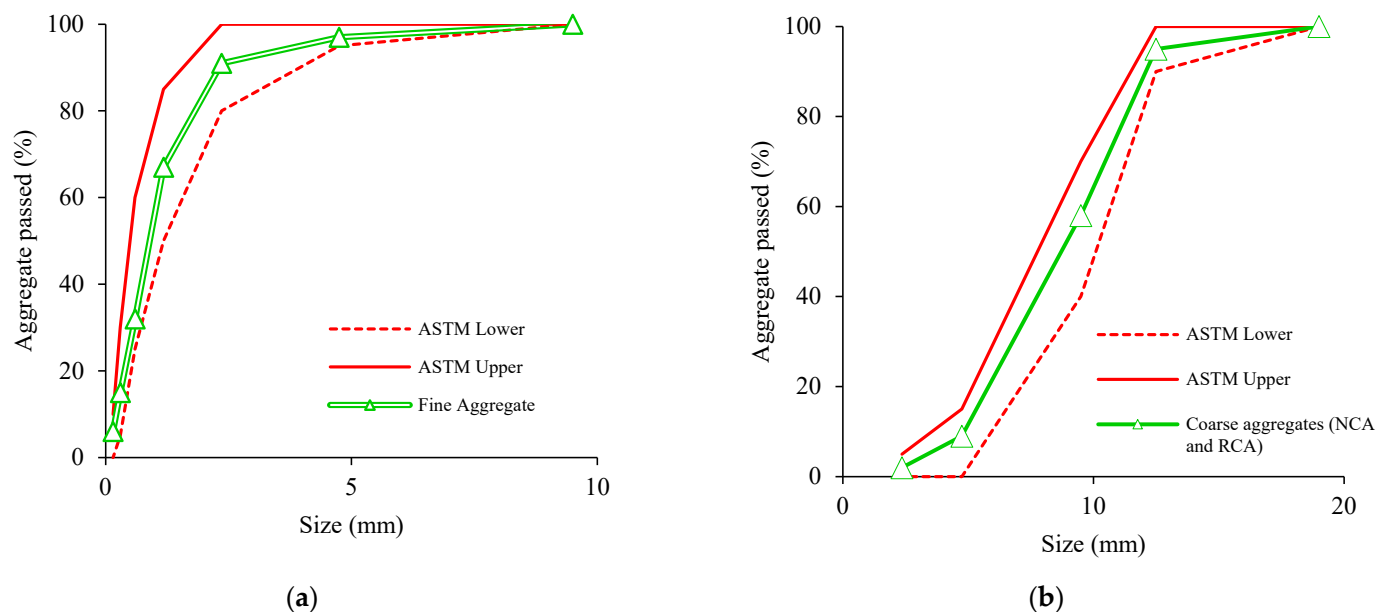


Figure 2. Aggregate gradation. (a) Fine aggregate. (b) Coarse aggregate.

2.1.3. Fiber Reinforcement

Steel chord wires of scrap tyres were manually shredded to prepare RTSF. The production of RTSF includes (1) manual extraction of chord wires from tyre waste, (2) burning of residual rubber particles to avoid the negative effect of weak rubber on the bond strength of RTSF, and (3) cleaned chord wires chopped into lengths varying between 25 mm and 37 mm. The density of RTSF is around 7700 kg/m³. Due to the use of high-quality raw steel in the tyre, RTSF possesses good ductility and a high tensile strength comparable to an artificial steel fiber (ASF) [44]. The RTSF sample is shown in Figure 3.



Figure 3. RTSF sample.

2.1.4. Plasticizer

For the mixing and curing of all mixtures, tap water was used. The effect of fibers on workability was minimized using a high-performance chemical admixture named Viscocrete 3110.

2.2. Details and Preparation of Concrete Mixtures

A total of thirteen mixes were investigated in this research, see Table 3. The first concrete mix “PNAC” was prepared with NCA to represent the control mix. After conducting trials, PNAC was designed as a high-performance concrete yielding slump of 200 ± 10 mm and f_{cm} of 70 MPa at 28 days. RAC was produced by complete replacement of NCA with RCA, to maximize the recycling of C&D waste. The complete details about proportioning of concrete ingredients are given in Table 3. A total of twelve RAC mixes were designed with various contents of MS and RTSF. MS was used as 0, 5, and 10% by volume substitution of cement. The incorporation levels of MS were decided by simultaneously considering the performance of concrete in fresh and hardened states [11,50] and the economy. With each level of MS, RAC was reinforced with the four different volume fractions of RTSF i.e., 0, 0.5, 1, and 2%. These doses of RTSF were selected to evaluate the effect of a wide range of fiber content on the mechanical performance of RAC. Superplasticizer (SP) was employed to maintain the desired workability at a low water-binder ratio of 0.3.

Table 3. Design of concrete mixtures.

Mix ID	RTSF (%)	MS (%)	Cement (kg/m ³)	MS (kg/m ³)	RTSF (kg/m ³)	Fine Aggregate (kg/m ³)	Coarse Aggregate (kg/m ³)	Water (kg/m ³)	SP (kg/m ³)
PNAC	0	0	505	0	0	812	935	151.5	2
RAC/R0	0	0	505	0	0	812	860	151.5	2
RAC/R0.5	0.5	0	505	0	39	806	854	151.5	2
RAC/R1	1	0	505	0	78	799	847	151.5	2.5
RAC/R2	2	0	505	0	156	786	834	151.5	2.5
RAC/R0/M5	0	5	480	19	0	812	860	151.5	2.5
RAC/R0.5/M5	0.5	5	480	19	39	806	854	151.5	3
RAC/R1/M5	1	5	480	19	78	799	847	151.5	3
RAC/R2/M5	2	5	480	19	156	786	834	151.5	3.5
RAC/R0/M10	0	10	455	37	0	812	860	151.5	3
RAC/R0.5/M10	0.5	10	455	37	39	806	854	151.5	3
RAC/R1/M10	1	10	455	37	78	799	847	151.5	3.5
RAC/R2/M10	2	10	455	37	156	786	834	151.5	3.5

The mixing of fresh batches was completed in four stages (1) Firstly, all solid ingredients were dry blended at 40 rpm speed for 2 min; (2) In the second stage, half the amount of SP and water were added to the dry mix, mixing has proceeded at 40 rpm for 2 min. (3) In the third stage, the remaining halves of SP and water were added to the mixer, and the mixing speed was increased to 60 rpm, and it lasted for 2 min. Plain mixes were processed in the three stages; however, fiber-reinforced mixes have proceeded for the fourth stage. (4) In the final/fourth stage, required quantities of fibers were added gradually to the plain fresh concrete, while mixing continued at a speed of 80 rpm for 4 min. After the completion of mixing, Abram's cone slump test was performed on all mixes according to ASTM C143 [51]. RAC mixes incorporating 0% and 0.5% RTSF showed slump values between 200–220 mm. While highly reinforced RAC mixes showed slump values between 130–200 mm. Three replicate samples of all mixes were made for the determination of a property at a given age. Samples were cast in the steel molds and kept for 24 h to set and eventually immersed for curing in the tap water.

2.3. Testing Methods

Several performance indicators of concrete such as f_{cm} , f_{ctm} , density, WA, ER, and UPV were evaluated to investigate the effects of MS and RTSF on RAC. For each type of parameter/property, three replicate samples of all mixes were tested at the specified ages, and their average result is reported in this research with standard deviation values. The f_{cm} of each mix was evaluated at the age of 7, 28, 90, and 180 days. For this purpose, 100 mm cubical specimens of concrete were tested according to ASTM C39 [52]. The f_{ctm} of all mixes was evaluated at the age of 28 and 90 days. For the splitting-tensile test, 100 × 200 mm cylindrical samples were prepared and tested according to ASTM C496 [53].

The density of each mix was measured to investigate the effect of RTSF and MS on the unit weight of RAC. For the evaluation of dry bulk density, 100 mm cubical samples were tested according to ASTM C948 [54]. The same samples were used to find out the WA capacity as per ASTM C948. The WA of each sample was measured at the age of 28 and 90-Days. To investigate the influence of RTSF and MS on the corrosion-risk potential of RAC, an ER test was performed on 100 mm cubical samples according to ASTM C1876 [55]. For the assessment of changes in the porosity of RAC due to the addition of RTSF and MS, an ultrasonic pulse velocity (UPV) test was conducted on 100 mm cubical samples according to ASTM C597 [56]. The ER and UPV of each mix were determined at the age of 28 and 90 days.

3. Results and Discussions

3.1. Density

The effect of MS and RTSF addition on the density of RAC is shown in Figure 4. As expected, the density decreased with the full replacement of NCA with RCA. This was because RCA had less dense or porous attached mortar which had a density lower than the natural aggregate. Therefore, RAC resulted in a 3.2% lower density than the PNAC. The addition of MS had shown a slight increase in the density of RAC. The particles of MS were smaller than that of the cement, therefore, MS can accommodate the spaces between cement particles and pores inside RCA. The filling effect of MS particles can improve the density of RAC [13]. Moreover, the addition of MS had the potential to reduce the free portlandite in the binder matrix and convert it into useful and dense calcium silicate hydrate (C-S-H) gel.

The addition of RTSF could cause a noticeable increment in the density of RAC for a given percentage of MS. At the addition of 2% RTSF, the density of RAC almost became equal to that of the PNAC. This was because the density of steel chords was about 3.5 times higher than that of plain concrete, therefore, a rising volume fraction of RTSF caused noticeable increments in the density. Therefore, RAC incorporating 10% MS and 2% RTSF exceeds in density compared to the PNAC mix.

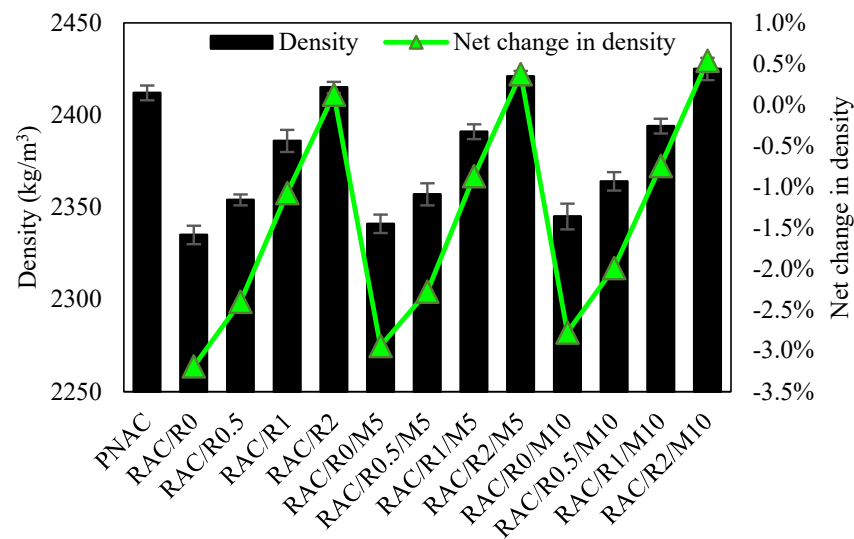


Figure 4. Effect of varying contents of MS and RTSF on the density of RAC.

3.2. Compressive Strength

The f_{cm} results of all mixes at 7, 28, 90, and 180 days are shown in Figure 5. The f_{cm} of RAC was around 15% lower than the PNAC. This is because plain RAC had a lower density than NAC. The voids present in the adhered mortar of RCA had a high amount of absorbed water in the saturated surface dry state. Therefore, the overall void content of RAC was high and could cause a reduction in the density and strength of concrete. Other than that, interfacial transition zones (ITZs) within RCA could play a negative role in reducing the strength of concrete [11], as ITZs acted as weak links in any concrete matrix under compressive loads. To elaborate, ITZs were regions where the properties of the RCA and the surrounding old cement paste were different. The ITZs were weaker than the rest of the concrete matrix, making them more prone to cracking or failure under stress.

MS addition caused notable improvements in the f_{cm} of RAC at the age of 90 and 180 days. The f_{cm} of RAC at 5% and 10% MS incorporation experienced an improvement of about 8 and 16%, respectively. At 10% MS incorporation, RAC showed f_{cm} similar to the PNAC. MS addition promoted the growth of CSH-gel, which could cause an increase in the strength of RAC, especially at later ages. Past literature [13,50] had reported that MS overcame the strength deficit of plain RAC compared to the PNAC. The ITZs between RCA and the binder matrix could also strengthen due to cross-reactions at ITZs between portlandite present in RCA and micro-silica particles in the binder matrix. Moreover, pores present inside RCA can also be penetrated by fine silica particles, which could also lead to the strengthening of ITZs between RCA and the binder matrix. Hence, MS addition could be beneficial to the strength of RAC.

The increase in RTSF content from 0 to 2% showed a mixed effect on the f_{cm} of RAC. The addition of 0.5 and 1% RTSF showed 4–6% increments in the f_{cm} , while the 2% RTSF addition showed no notable change in the f_{cm} . The changing behavior of f_{cm} with the rising fiber content could be explained as fiber-reinforcement affected the f_{cm} in two opposite ways (1) confinement effect and control over the premature cracking and brittle failure may contribute positively to the strength [23,26] (2) while poor dispersion may lead to the increase in air voids of concrete detrimental to the f_{cm} [57]. It was hypothesized that at a high fiber volume, the accumulation of RTSF filaments could cause a reduction in the utilization of fibers. Previous studies [44,45] confirmed that RTSF incorporation of up to 1% volume fraction can increase the f_{cm} by up to 5–8%.

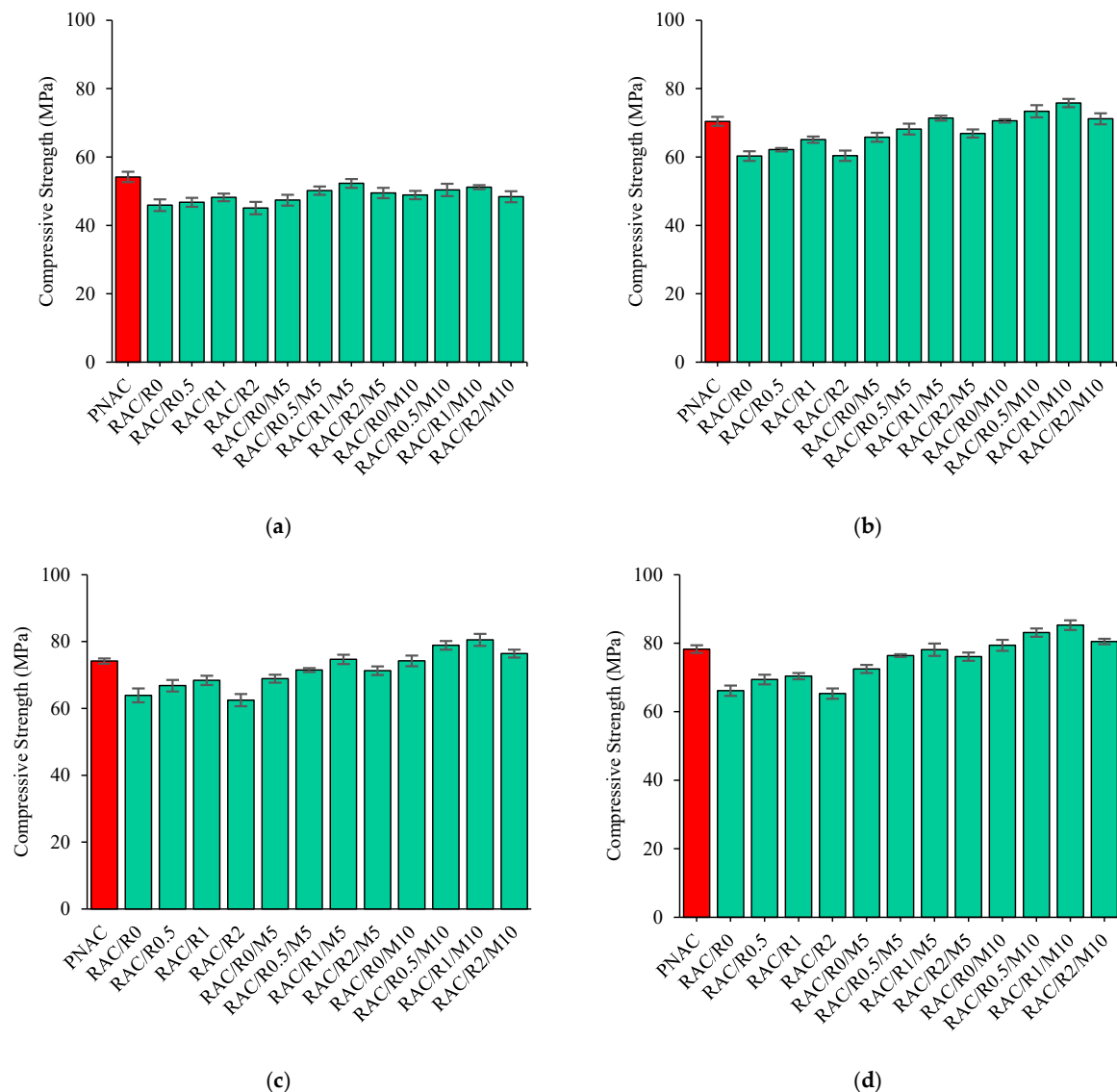


Figure 5. Compressive strength (f_{cm}) of RAC with the varying content of MS and RTSF at the age of (a) 7-Days (b) 28-Days (c) 90-Days and (d) 180-Days.

Simultaneous incorporation of MS and RTSF led to noticeable improvements of 18–29% in the f_{cm} of RAC compared to plain RAC (i.e., RAC/R0). Mixes containing 5% MS and 1% RTSF showed f_{cm} similar to the PNAC. While mixes made with 10% MS and all RTSF (0.5, 1, and 1.5%) contents showed higher strength compared to PNAC. Among all mixtures, the maximum f_{cm} , 7.6–8.5% higher than PNAC, was shown by RAC made with 10% MS and 1% RTSF. The MS incorporation seems to improve the strength of the matrix through the filler effect and pozzolanic reaction, while RTSF could improve the strength by offering crack resistance. The maximum contribution of MS in RAC was noticed at the age of 180 days. This could be because the pozzolanic reaction between silica particles and portlandite was slow and took a long duration. At the age of 180 days, the f_{cm} of RAC increased by about 20% at the addition of 10%. Moreover, MS addition also seemed to increase the efficiency of RTSF. For example, mixes incorporating MS showed more net achievement in the f_{cm} due to 1% RTSF than the mixes without MS. This can be related to the improvement in dispersion and bond of RTSF with plain matrix owing to improved strength and dense packing of binder particles with MS addition. The improvement in the efficiency of artificial steel fibers with MS addition was also noted in previous study [50]. The strengthening of the binder improved the bond performance of fiber filaments and plain matrix [58].

3.3. Splitting Tensile Strength

The f_{ctm} of the PNAC mix and RAC with different contents of MS and RTSF is shown in Figure 6. Complete substitution of NCA with RCA showed a reduction of 13% in f_{ctm} . This seemed to be the result of the low-density mortar present in RCA. Previous studies [26,44,45] reported a decline of around 15–20% in f_{ctm} when RCA was used as a full replacement for NCA. MS led to notable increments in the f_{ctm} of RAC. At 28 days, the tensile strength of RAC was increased by 9% and 8.3% at 5% MS and 10% MS incorporation, respectively. While, at 90 days, RAC experienced increments of 13% and 14.7% respectively due to 5% and 10% MS addition. The high percentage of MS (i.e., 10%) showed a major contribution to the tensile strength at 90 days due to the slow development of C-S-H in pozzolanic reactions. The plain mix of RAC containing 10% MS showed tensile strength comparable to that of the PNAC mix. MS addition could result in the strengthening of the plain matrix and improve the bond between the RCA and binder matrix of RAC [11]. This may have resulted in the improvement of the tensile strength of plain RAC.

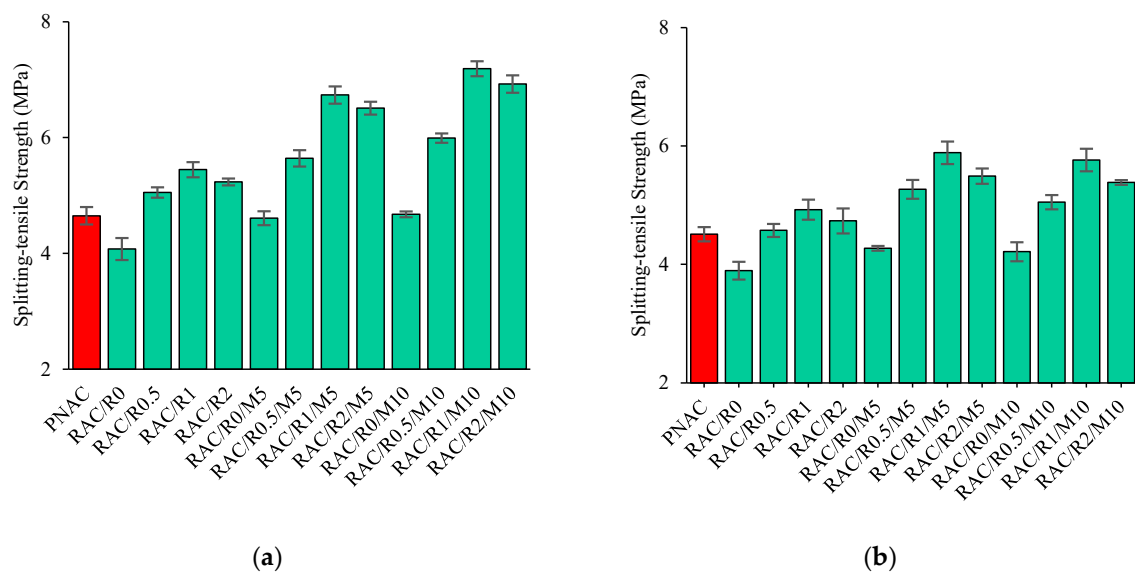


Figure 6. Effect of varying contents of MS and RTSF on the f_{ctm} of RAC at the age of (a) 28 and (b) 90-days.

Compared to MS, RTSF showed a substantial increase in the f_{ctm} of plain RAC. At 28 days, RTSF incorporation at 0.5, 1, and 1.5% volume fractions correspondingly caused increments of 17, 26, and 23% in the f_{ctm} of plain RAC. While at 90 days, the efficiency of RTSF was further improved notably, for example, 0.5, 1, and 2% RTSF contents caused f_{ctm} of RAC to increase by 23%, 33%, and 28%, respectively. As the concrete aged, it seemed to strengthen the binder matrix hence the bond between fibers and concrete could also strengthen, which may have resulted in the increased efficiency of RTSF. Available studies have [59,60] reported the tensile strength increase of about 20–30% at 1.5% incorporation of shredded RTSF. The efficiency of RTSF declined at a 2% volume fraction and it seemed to be related to the increase in porosity or air voids due to lack of proper dispersion of fiber filaments at a high fiber volume [50].

Figure 7 shows the f_{ctm} of RAC with various levels of RTSF and MS relative to the PNAC. High-level net gains in the f_{ctm} of RAC were noticed when RTSF was incorporated along with MS. For example, 1% RTSF addition showed about a 40% increase in the f_{ctm} of RAC when used in conjunction with 5% MS, while it showed about 26% increase in the f_{ctm} when used without MS. Similar improvements were noticed with other combinations of MS and RTSF as well. Thus, MS could increase the utilization of RTSF towards the ductility of RAC. The improvement in fiber efficiency with MS addition could be credited to the increased bond strength at the ITZs between fiber filaments and plain matrix. The

strengthening of the bond seemed to be effective and ensured the high pull-out strength of fibers in binders containing MS [58]. The results of f_{ctm} also highlighted the importance of RTSF alone, which can notably change the tensile strength even at 0.5% volume fraction. All RAC mixes incorporating RTSF showed higher tensile strength than PNAC at both ages of testing. Furthermore, conjunctive addition of MS with RTSF could lead to RAC with possibly high tensile strength than PNAC. As can be noted in Figure 8, RAC containing 1% RTSF and 5–10% MS outperformed PNAC by exhibiting 38–41% more f_{ctm} .

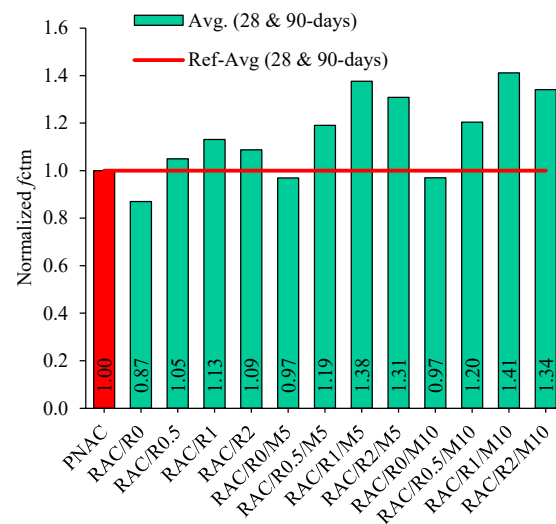


Figure 7. Variation of normalized f_{ctm} (f_{ctm_mix}/f_{ctm_PNAC}) with changing RTSF and MS contents.

3.4. Water Absorption

The effect of MS and RTSF contents on the WA capacity of RAC is shown in Figure 8. WA measures the permeable porosity of concrete which is an indirect assessment of durability against the ingress of harmful substances into concrete. The results showed RAC had an 18–23% higher WA than that of the PNAC mix. This notable increase in the WA capacity could be attributed to the presence of adhered mortar on the surface of the RCA particles. The inclusion of RCA as a replacement for natural coarse aggregate could increase both pore connectivity and pore volume.

The inclusion of MS can notably reduce the WA capacity of RAC. For example, 5% and 10% MS addition caused 33% and 45% reductions in the WA capacity of RAC, respectively. As MS has extremely fine particles compared to cement, therefore, it could have efficiently increased the imperviousness of the plain matrix. Besides that, MS particles can also reduce the permeation of water along the weak ITZs between RCA and the binder matrix. The presence of fine particles of MS seems to be the tortuosity of permeable paths within a material, which ultimately may lead to the creation of an impermeable microstructure [18]. This is worth mentioning here, that RAC with 5% MS showed a 10% lower WA capacity than that of the PNAC mix at 90 days. Whereas RAC with 10% MS showed a 15% and 22% reduction in WA w.r.t PNAC mix at the age of 28 and 90 days, respectively. Thus, MS could notably control the negative effect of RCA on imperviousness.

The addition of RTSF without MS showed mixed effects on the WA capacity of RAC. Initially, WA was reduced at 0.5% RTSF, then absorption capacity started increasing with a further rise in RTSF compared to plain RAC and the maximum WA was observed at 2% RTSF. The positive effect of a small volume of fibers could be credited to the increased control of fibers over the aggregate sinking, and slurry flow which may eventually reduce cracks due to the drying shrinkage [61]. Alsaiif et al. [62] reported that using artificial steel fibers could result in a 13% decline in the WA capacity of concrete. While at a high volume of fibers, the difficulty in compaction and improper dispersion issue could increase the void pockets in the concrete and it eventually caused the WA increase [19]. Mixes of RAC with combined incorporation of MS and RTSF showed smaller WA capacity as compared

to PNAC mix except for the RAC with 5% MS and 2% RTSF (RAC/R2/M5). The influence of MS was found to be dominant to reduce the WA in the mixes with both MS and RTSF. RAC with 10% MS and all contents of RTSF can yield notably lower WA than that of the PNAC mix.

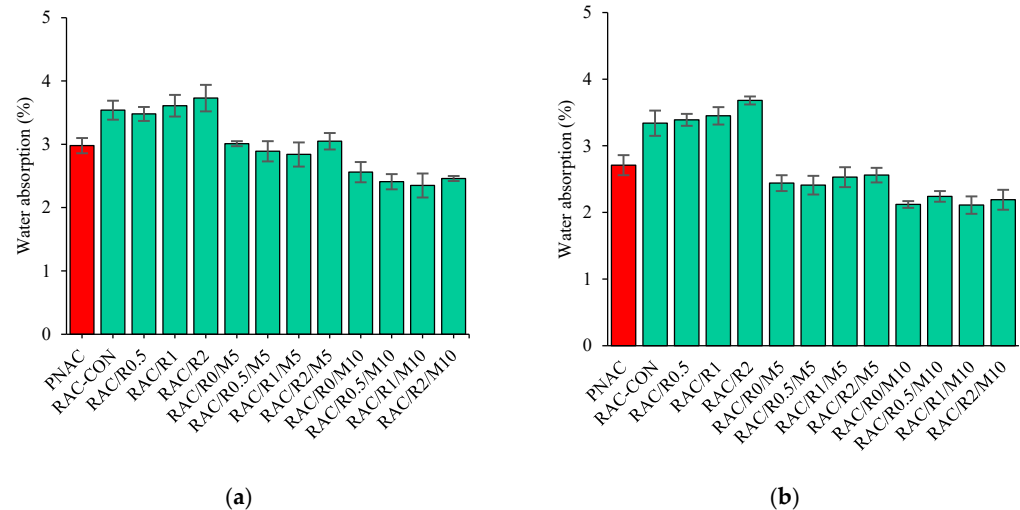


Figure 8. Effect of RTSF and MS on WA capacity of RAC measured at (a) 28 days, and (b) 90-days.

3.5. Ultrasonic Pulse Velocity (km/s)

Changes in homogeneity and porosity of concrete can be assessed by the UPV test. The effect of RTSF and MS contents on the UPV of RAC was shown in Figure 9. All UPV values were pertaining to concretes of high strength and good quality as no experimental UPV value was below 3500 m/s. Since RCA had high porosity than NCA, RAC showed a lower UPV value than the PNAC mix. The possible porosity increase delayed the time of travel of pulse waves from a transmitter to the receiver poles of the UPV test apparatus. However, MS addition could cause an increase in the UPV of concrete. This indicated that the homogeneity and imperviousness of RAC can be increased with MS incorporation. Similar to the present study, Kou et al. [11] reported that UPV gain of RAC was increased with MS addition. Fine MS particles may consume free portlandite, strengthened the binder matrix, and bond between RCA and the binder matrix. The reduction in the distance between particles and improved packing of constituent particles could also cause gains of UPV in RAC mixes.

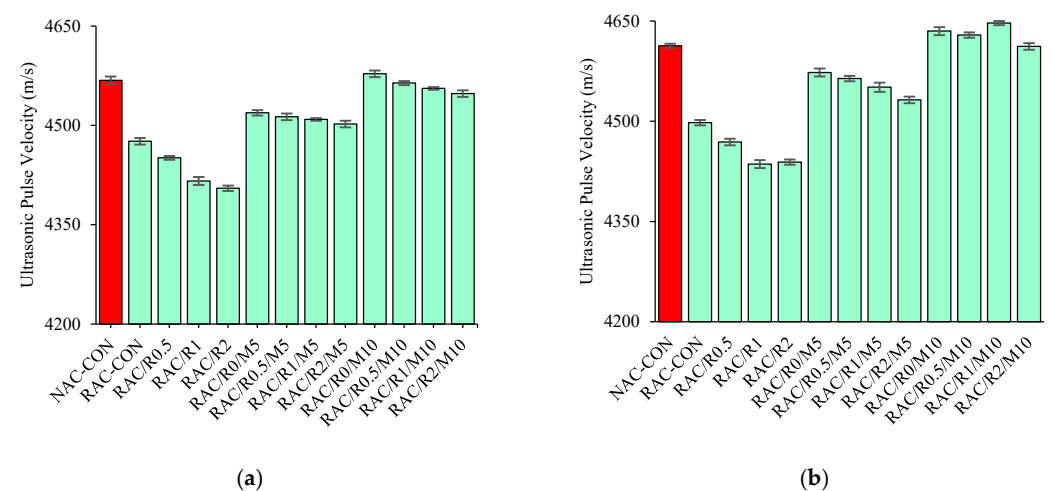


Figure 9. Effect of varying contents of MS and RTSF on UPV of RAC at the age of (a) 28 and (b) 90-days.

Unlike MS, RTSF incorporation showed a decline in UPV. Although RTSF had a high density, it cannot notably change the porosity of the plain matrix. Besides that, fiber filaments seemed to introduce heterogeneity in the RAC matrix and could possibly cause UPV to decline. Fibers oriented in a different direction may also deflect the pulse waves slowing the propagation time of pulse waves. Yazici et al. [63] noted that the addition of steel fiber can cause a 1–9% decline in the UPV of concrete when fiber content was increased from 0.5 to 1.5%. This could have been caused by the increase in the porosity due to the increasing difficulty in compaction with the rise in fiber content. A major decline in UPV due to RTSF was noticed in RAC without MS. While minor UPV decline was observed in RAC with MS. The interaction of the binder matrix with RTSF may be poor when MS was not used. This may create more voids due to RTSF incorporation in mixes without MS. On the other hand, fine MS particles can ensure a strong interaction between the binder phase and fiber filaments. Thus, the intensity of the negative effect of RTSF on the void ratio could be minimized with the application of MS. A little UPV change due to RTSF variation in MS-containing mixes also indicated that the mineral admixture incorporation improved the dispersion of fiber filaments.

3.6. Electrical Resistivity

The durability of steel-reinforced concrete against corrosion can be estimated via different techniques. ER is a non-destructive evaluation that allows a simple assessment of the corrosion risk potential of concrete according to existing classifications [64]. The variation of ER of RAC against different contents of RTSF and MS is shown in Figure 10.

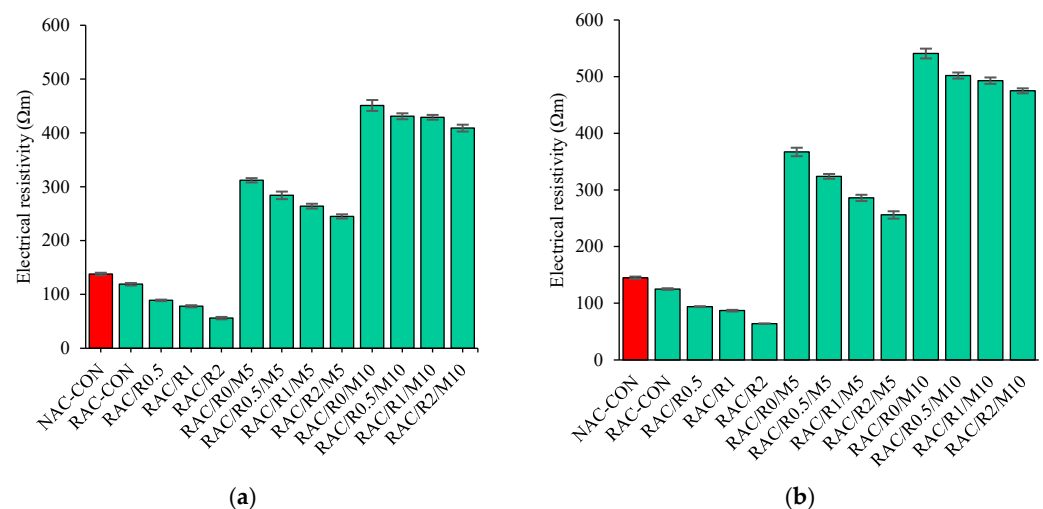


Figure 10. Effect of RTSF and MS contents on ER of RAC measured at (a) 28-days and (b) 90-days.

It was observed that RAC had a lower ER than that of the PNAC mix. This can be caused by the presence of high porosity in RCA which facilitates penetration of ions. Also, a high amount of moisture in RAC allowed faster penetration of electricity [65]. However, RAC showed ER values around 120 Ωm that pertains to concrete with ‘no probability’ of corrosion [64]. This may be credited to the low-water binder ratio used to develop the high-strength concrete in this study. While mixes with ER values of 120 to 50 Ωm and below 50 Ωm had a ‘probable risk to rebar corrosion’ and ‘vulnerable to rebar corrosion’, respectively [64]. Thus, RAC containing RTSF without MS had a ‘probable risk’ of corrosion. The ER was reduced further, with the rise in RTSF content. This could be blamed on the high electrical conductivity of steel fibers. While a mild increase in the porosity of concrete due to high fiber volumes can also lead to an increase in the corrosion risk potential of concrete [66]. Afroughsabet et al. [25] reported that the ER value of concrete was reduced from 75 to 20 Ωm upon the addition of 1% volume of steel fiber.

The addition of 5% and 10% MS had proven extremely useful in increasing the ER of RAC. In other words, the corrosion-risk potential of RAC can be minimized considerably

by incorporating MS in the binder. The pozzolanic influence of MS may reduce the free portlandite and produce secondary C-S-H gel. MS seemed to help in producing a dense microstructure that disrupted the free movement of ions present in pore solution triggered by electrical currents. Kou et al. [67] reported that the ingress of chloride ions was interrupted due to the incorporation of pozzolanic admixtures (i.e., MS, fly ash, and slag). The ER of RAC/R0/M5 and RAC/R0/M10 was about 2.2 and 3.3 times higher than that of the PNAC mix. Thus, the studied RAC made with 5% or 10% MS addition had no probable risk of corrosion.

The manufacture of steel fiber-reinforced RAC made with RTSF having a 'low' or 'no probable' risk of corrosion was achieved with the application of MS. The noticeable reduction in the porosity, as indicated by the results of WA, reduced the penetration of electrical current and compensates for the high electrical conductivity of steel fibers. It is also worth mentioning here that, although ER was a quick and convenient measure of the corrosion-risk potential of concrete, it can overestimate the influence of steel fibers on the corrosion risk of concrete [19]. Therefore, a reliable assessment of the corrosion risk potential of steel fiber-reinforced concrete can only be made by conducting a chloride ion diffusion test or immersion method [68]. As steel fibers caused little change in porosity [14], therefore, they are also anticipated to show little influence on the chloride-ion penetration resistance of concrete.

4. Conclusions

This paper studied the effect of different RTSF and MS contents on the mechanical and physical parameters of RAC at different ages. The following key findings can be drawn from experimental results:

- The overall density of RAC may be increased by the incorporation of both RTSF and MS. However, the increase in fiber content could increase the voids/pore connectivity in the plain concrete matrix. Seemingly, owing to the filling action and pozzolanicity, MS addition showed minor improvements in the density of concrete.
- The optimum dosage of RTSF can be taken as '1%' considering the maximum improvement in f_{cm} and f_{ctm} . RAC made with 10% MS and 1% RTSF could show 7.6–8.5% higher f_{cm} compared to PNAC.
- The f_{ctm} of RAC with all contents of RTSF was found to be higher compared to the PNAC. At the age of 90 days, RAC made with 10% MS and 1% RTSF could result in 54% more f_{ctm} than PNAC. MS inclusion could result in improvement in the utilization of RTSF towards the ductility of RAC. The increased fiber efficiency with MS addition seemed to be linked with the increased bond strength at the ITZs between fiber filaments and plain matrix.
- Even though 2% RTSF did not cause a noticeable improvement in mechanical performance but samples with 2% RTSF can yield showed smaller crack widths after peak load than samples with low levels of RTSF.
- The efficiency of RTSF can be increased by improving the mechanical properties with MS incorporation and increase in age.
- The UPV of RAC was slightly reduced due to the RTSF addition. Therefore, UPV could not be taken as a good measure to estimate the mechanical properties of steel fiber-reinforced concretes.
- Fine MS particles can ensure a strong interaction between the binder phase and fiber filaments. Thus, the intensity of the negative effect of RTSF on the void ratio can be minimized with the application of MS.
- The absorption capacity of RAC notably can be decreased due to MS addition. At 10% MS addition, RAC exhibited 15–23% lower WA than PNAC.
- The corrosion-risk potential of RAC could increase with RTSF incorporation. While MS could notably enhance the ER of RAC. The corrosion-risk potential of RAC made with 5 and 10% MS was 'not probable'. MS seemed to be effective in controlling the corrosion resistance of RAC made with RTSF.

Author Contributions: Conceptualization, M.T.A., H.A. and S.S.R.; methodology, H.A.; software, S.R.; validation, S.R., A.A.A.S. and S.A.; formal analysis, M.T.A.; investigation, S.R.; resources, S.R.; data curation, M.T.A.; writing—original draft preparation, M.T.A.; writing—review and editing, A.A.A.S.; visualization, S.A.; supervision, H.A., S.S.R. and S.A.; project administration, S.R.; funding acquisition, A.A.A.S. All authors have read and agreed to the published version of the manuscript.

Funding: The authors extend their appreciation to the Deanship of Scientific Research at King Khalid University for funding this work through large group Research Project under grant number R.G.P. 2/351/44.

Data Availability Statement: All data used is available in this research paper.

Acknowledgments: The authors extend their appreciation to the Deanship of Scientific Research at King Khalid University for funding this work through large group Research Project under grant number R.G.P. 2/351/44.

Conflicts of Interest: The authors declare no conflict of interest.

References

1. Akhtar, A.; Sarmah, A.K. Construction and Demolition Waste Generation and Properties of Recycled Aggregate Concrete: A Global Perspective. *J. Clean. Prod.* **2018**, *186*, 262–281. [\[CrossRef\]](#)
2. Kurda, R.; Silvestre, J.D.; de Brito, J. Life Cycle Assessment of Concrete Made with High Volume of Recycled Concrete Aggregates and Fly Ash. *Resour. Conserv. Recycl.* **2018**, *139*, 407–417. [\[CrossRef\]](#)
3. Şahmaran, M.; Li, V.C. Durability Properties of Micro-Cracked ECC Containing High Volumes Fly Ash. *Cem. Concr. Res.* **2009**, *39*, 1033–1043. [\[CrossRef\]](#)
4. Strieder, H.L.; Dutra, V.F.P.; Graeff, Â.G.; Núñez, W.P.; Merten, F.R.M. Performance Evaluation of Pervious Concrete Pavements with Recycled Concrete Aggregate. *Constr. Build. Mater.* **2022**, *315*, 125384. [\[CrossRef\]](#)
5. Hoffmann, C.; Schubert, S.; Leemann, A.; Motavalli, M. Recycled Concrete and Mixed Rubble as Aggregates: Influence of Variations in Composition on the Concrete Properties and Their Use as Structural Material. *Constr. Build. Mater.* **2012**, *35*, 701–709. [\[CrossRef\]](#)
6. Shi, X.; Mukhopadhyay, A.; Zollinger, D.; Grasley, Z. Economic Input-Output Life Cycle Assessment of Concrete Pavement Containing Recycled Concrete Aggregate. *J. Clean. Prod.* **2019**, *225*, 414–425. [\[CrossRef\]](#)
7. Kurad, R.; Silvestre, J.D.; de Brito, J.; Ahmed, H. Effect of Incorporation of High Volume of Recycled Concrete Aggregates and Fly Ash on the Strength and Global Warming Potential of Concrete. *J. Clean. Prod.* **2017**, *166*, 485–502. [\[CrossRef\]](#)
8. Kurda, R.; Silvestre, J.D.; de Brito, J. Toxicity and Environmental and Economic Performance of Fly Ash and Recycled Concrete Aggregates Use in Concrete: A Review. *Heliyon* **2018**, *4*, e00611. [\[CrossRef\]](#)
9. Maia, M.B.; De Brito, J.; Martins, I.M.; Silvestre, J.D. Toxicity of Recycled Concrete Aggregates: Review on Leaching Tests. *Open Constr. Build. Technol. J.* **2018**, *12*, 187–196. [\[CrossRef\]](#)
10. Kurda, R.; de Brito, J.; Silvestre, J.D. Influence of Recycled Aggregates and High Contents of Fly Ash on Concrete Fresh Properties. *Cem. Concr. Compos.* **2017**, *84*, 198–213. [\[CrossRef\]](#)
11. Kou, S.; Poon, C.; Agrela, F. Comparisons of Natural and Recycled Aggregate Concretes Prepared with the Addition of Different Mineral Admixtures. *Cem. Concr. Compos.* **2011**, *33*, 788–795. [\[CrossRef\]](#)
12. Lam, C.S.; Poon, C.S.; Chan, D. Enhancing the Performance of Pre-Cast Concrete Blocks by Incorporating Waste Glass—ASR Consideration. *Cem. Concr. Compos.* **2007**, *29*, 616–625. [\[CrossRef\]](#)
13. Dilbas, H.; Şimşek, M.; Çakır, Ö. An Investigation on Mechanical and Physical Properties of Recycled Aggregate Concrete (RAC) with and without Silica Fume. *Constr. Build. Mater.* **2014**, *61*, 50–59. [\[CrossRef\]](#)
14. Koushkbaghi, M.; Kazemi, M.J.; Mosavi, H.; Mohseni, E. Acid Resistance and Durability Properties of Steel Fiber-Reinforced Concrete Incorporating Rice Husk Ash and Recycled Aggregate. *Constr. Build. Mater.* **2019**, *202*, 266–275. [\[CrossRef\]](#)
15. Xie, J.; Fang, C.; Lu, Z.; Li, Z.; Li, L. Effects of the Addition of Silica Fume and Rubber Particles on the Compressive Behaviour of Recycled Aggregate Concrete with Steel Fibres. *J. Clean. Prod.* **2018**, *197*, 656–667. [\[CrossRef\]](#)
16. He, W.; Kong, X.; Fu, Y.; Zhou, C.; Zheng, Z. Experimental Investigation on the Mechanical Properties and Microstructure of Hybrid Fiber Reinforced Recycled Aggregate Concrete. *Constr. Build. Mater.* **2020**, *261*, 120488. [\[CrossRef\]](#)
17. Kazmi, S.M.S.; Munir, M.J.; Wu, Y.-F.; Patnaikuni, I.; Zhou, Y.; Xing, F. Axial Stress-Strain Behavior of Macro-Synthetic Fiber Reinforced Recycled Aggregate Concrete. *Cem. Concr. Compos.* **2019**, *97*, 341–356. [\[CrossRef\]](#)
18. Kurda, R.; de Brito, J.; Silvestre, J.D. Water Absorption and Electrical Resistivity of Concrete with Recycled Concrete Aggregates and Fly Ash. *Cem. Concr. Compos.* **2019**, *95*, 169–182. [\[CrossRef\]](#)
19. Ali, B.; Raza, S.S.; Kurda, R.; Alyousef, R. Synergistic Effects of Fly Ash and Hooked Steel Fibers on Strength and Durability Properties of High Strength Recycled Aggregate Concrete. *Resour. Conserv. Recycl.* **2021**, *168*, 105444. [\[CrossRef\]](#)
20. Çakır, Ö.; Sofyanlı, Ö.Ö. Influence of Silica Fume on Mechanical and Physical Properties of Recycled Aggregate Concrete. *HBRC J.* **2015**, *11*, 157–166. [\[CrossRef\]](#)
21. Sasanipour, H.; Aslani, F.; Taherinezhad, J. Chloride Ion Permeability Improvement of Recycled Aggregate Concrete Using Pretreated Recycled Aggregates by Silica Fume Slurry. *Constr. Build. Mater.* **2021**, *270*, 121498. [\[CrossRef\]](#)

22. Dimitriou, G.; Savva, P.; Petrou, M.F. Enhancing Mechanical and Durability Properties of Recycled Aggregate Concrete. *Constr. Build. Mater.* **2018**, *158*, 228–235. [[CrossRef](#)]
23. Ali, B.; Qureshi, L.A.; Khan, S.U. Flexural Behavior of Glass Fiber-Reinforced Recycled Aggregate Concrete and Its Impact on the Cost and Carbon Footprint of Concrete Pavement. *Constr. Build. Mater.* **2020**, *262*, 120820. [[CrossRef](#)]
24. Kazmi, S.M.S.; Munir, M.J.; Wu, Y.-F.; Patnaikuni, I. Effect of Macro-Synthetic Fibers on the Fracture Energy and Mechanical Behavior of Recycled Aggregate Concrete. *Constr. Build. Mater.* **2018**, *189*, 857–868. [[CrossRef](#)]
25. Afrouhsabet, V.; Biolzi, L.; Ozbakkaloglu, T. Influence of Double Hooked-End Steel Fibers and Slag on Mechanical and Durability Properties of High Performance Recycled Aggregate Concrete. *Compos. Struct.* **2017**, *181*, 273–284. [[CrossRef](#)]
26. Das, C.S.; Dey, T.; Dandapat, R.; Mukharjee, B.B.; Kumar, J. Performance Evaluation of Polypropylene Fibre Reinforced Recycled Aggregate Concrete. *Constr. Build. Mater.* **2018**, *189*, 649–659. [[CrossRef](#)]
27. Ali, B.; Qureshi, L.A.; Shah, S.H.A.; Rehman, S.U.; Hussain, I.; Iqbal, M. A Step towards Durable, Ductile and Sustainable Concrete: Simultaneous Incorporation of Recycled Aggregates, Glass Fiber and Fly Ash. *Constr. Build. Mater.* **2020**, *251*, 118980. [[CrossRef](#)]
28. Mastali, M.; Dalvand, A. Use of Silica Fume and Recycled Steel Fibers in Self-Compacting Concrete (SCC). *Constr. Build. Mater.* **2016**, *125*, 196–209. [[CrossRef](#)]
29. Wang, L.E.I.; Guo, F.; Yang, H.; Wang, Y.A.N.; Tang, S. Comparison of Fly Ash, PVA Fiber, MgO and Shrinkage-Reducing Admixture on the Frost Resistance of Face Slab Concrete via Pore Structural and Fractal Analysis. *Fractals* **2021**, *29*, 2140002. [[CrossRef](#)]
30. Wang, L.; Zeng, X.; Li, Y.; Yang, H.; Tang, S. Influences of MgO and PVA Fiber on the Abrasion and Cracking Resistance, Pore Structure and Fractal Features of Hydraulic Concrete. *Fractal Fract.* **2022**, *6*, 674. [[CrossRef](#)]
31. Zarei, A.; Rooholamini, H.; Ozbakkaloglu, T. Evaluating the Properties of Concrete Pavements Containing Crumb Rubber and Recycled Steel Fibers Using Response Surface Methodology. *Int. J. Pavement Res. Technol.* **2022**, *15*, 470–484. [[CrossRef](#)]
32. Papachristoforou, M.; Anastasiou, E.K.; Papayianni, I. Durability of Steel Fiber Reinforced Concrete with Coarse Steel Slag Aggregates Including Performance at Elevated Temperatures. *Constr. Build. Mater.* **2020**, *262*, 120569. [[CrossRef](#)]
33. Ali, B.; Raza, S.S.; Hussain, I.; Iqbal, M. Influence of Different Fibers on Mechanical and Durability Performance of Concrete with Silica Fume. *Struct. Concr.* **2020**; *in press*. [[CrossRef](#)]
34. Ali, B.; Qureshi, L.A.; Kurda, R. Environmental and Economic Benefits of Steel, Glass, and Polypropylene Fiber Reinforced Cement Composite Application in Jointed Plain Concrete Pavement. *Compos. Commun.* **2020**, *22*, 100437. [[CrossRef](#)]
35. Xie, J.; Zhang, Z.; Lu, Z.; Sun, M. Coupling Effects of Silica Fume and Steel-Fiber on the Compressive Behaviour of Recycled Aggregate Concrete after Exposure to Elevated Temperature. *Constr. Build. Mater.* **2018**, *184*, 752–764. [[CrossRef](#)]
36. Chan, R.; Santana, M.A.; Oda, A.M.; Paniguel, R.C.; Vieira, L.B.; Figueiredo, A.D.; Galobardes, I. Analysis of Potential Use of Fibre Reinforced Recycled Aggregate Concrete for Sustainable Pavements. *J. Clean. Prod.* **2019**, *218*, 183–191. [[CrossRef](#)]
37. Hu, H.; Papastergiou, P.; Angelakopoulos, H.; Guadagnini, M.; Pilakoutas, K. Mechanical Properties of SFRC Using Blended Recycled Tyre Steel Cords (RTSC) and Recycled Tyre Steel Fibres (RTSF). *Constr. Build. Mater.* **2018**, *187*, 553–564. [[CrossRef](#)]
38. Zhong, H.; Zhang, M. Experimental Study on Engineering Properties of Concrete Reinforced with Hybrid Recycled Tyre Steel and Polypropylene Fibres. *J. Clean. Prod.* **2020**, *259*, 120914. [[CrossRef](#)]
39. Revuelta, D.; Carballosa, P.; García Calvo, J.L.; Pedrosa, F. Residual Strength and Drying Behavior of Concrete Reinforced with Recycled Steel Fiber from Tires. *Materials* **2021**, *14*, 6111. [[CrossRef](#)]
40. Khan, M.; Rehman, A.; Ali, M. Efficiency of Silica-Fume Content in Plain and Natural Fiber Reinforced Concrete for Concrete Road. *Constr. Build. Mater.* **2020**, *244*, 118382. [[CrossRef](#)]
41. Islam, M.S.; Ahmed, S.J.U. Influence of Jute Fiber on Concrete Properties. *Constr. Build. Mater.* **2018**, *189*, 768–776. [[CrossRef](#)]
42. Liew, K.M.; Akbar, A. The Recent Progress of Recycled Steel Fiber Reinforced Concrete. *Constr. Build. Mater.* **2020**, *232*, 117232. [[CrossRef](#)]
43. Aiello, M.A.; Leuzzi, F.; Centonze, G.; Maffezzoli, A. Use of Steel Fibres Recovered from Waste Tyres as Reinforcement in Concrete: Pull-out Behaviour, Compressive and Flexural Strength. *Waste Manag.* **2009**, *29*, 1960–1970. [[CrossRef](#)] [[PubMed](#)]
44. Ahmadi, M.; Farzin, S.; Hassani, A.; Motamedi, M. Mechanical Properties of the Concrete Containing Recycled Fibers and Aggregates. *Constr. Build. Mater.* **2017**, *144*, 392–398. [[CrossRef](#)]
45. Moghadam, A.S.; Omidinasab, F.; Abdalikia, M. The Effect of Initial Strength of Concrete Wastes on the Fresh and Hardened Properties of Recycled Concrete Reinforced with Recycled Steel Fibers. *Constr. Build. Mater.* **2021**, *300*, 124284. [[CrossRef](#)]
46. ASTM-C150; Standard Specification for Portland Cement. ASTM International: West Conshohocken, PA, USA, 2018.
47. ASTM C33/C33M-18; Standard Specification for Concrete Aggregates. ASTM International: West Conshohocken, PA, USA, 2018.
48. ASTM-C127; Standard Test Method for Relative Density (Specific Gravity) and Absorption of Coarse Aggregate. ASTM International: West Conshohocken, PA, USA, 2015.
49. ASTM-C128; Standard Test Method for Density, Relative Density (Specific Gravity), and Absorption of Fine Aggregate. ASTM International: West Conshohocken, PA, USA, 2001.
50. Raza, S.S.; Ali, B.; Noman, M.; Fahad, M.; Elhadi, K.M. Mechanical Properties, Flexural Behavior, and Chloride Permeability of High-Performance Steel Fiber-Reinforced Concrete (SFRC) Modified with Rice Husk Ash and Micro-Silica. *Constr. Build. Mater.* **2022**, *359*, 129520. [[CrossRef](#)]

51. ASTM-C143; Standard Test Method for Slump of Hydraulic-Cement Concrete. ASTM International: West Conshohocken, PA, USA, 2015.
52. ASTM C39/C39M-12; Standard Test Method for Compressive Strength of Cylindrical Concrete Specimens. ASTM International: West Conshohocken, PA, USA, 2012.
53. ASTM-C496; Standard Test Method for Splitting Tensile Strength of Cylindrical Concrete Specimens. ASTM International: West Conshohocken, PA, USA, 2017.
54. ASTM-C948; Standard Test Method for Dry and Wet Bulk Density, Water Absorption, and Apparent Porosity of Thin Sections of Glass-Fiber Reinforced Concrete. ASTM International: West Conshohocken, PA, USA, 2016.
55. ASTM C1876-19; Standard Test Method for Bulk Electrical Resistivity or Bulk Conductivity of Concrete. ASTM International: West Conshohocken, PA, USA, 2019. Available online: <https://www.astm.org/c1876-19.html> (accessed on 5 September 2020).
56. ASTM C597-16; Standard Test Method for Pulse Velocity through Concrete. ASTM International: West Conshohocken, PA, USA, 2016. Available online: <https://www.astm.org/c0597-16.html> (accessed on 5 September 2020).
57. Xie, J.; Guo, Y.; Liu, L.; Xie, Z. Compressive and Flexural Behaviours of a New Steel-Fibre-Reinforced Recycled Aggregate Concrete with Crumb Rubber. *Constr. Build. Mater.* **2015**, *79*, 263–272. [[CrossRef](#)]
58. Wu, Z.; Shi, C.; Khayat, K.H. Influence of Silica Fume Content on Microstructure Development and Bond to Steel Fiber in Ultra-High Strength Cement-Based Materials (UHSC). *Cem. Concr. Compos.* **2016**, *71*, 97–109. [[CrossRef](#)]
59. Simalti, A.; Singh, A.P. Comparative Study on Performance of Manufactured Steel Fiber and Shredded Tire Recycled Steel Fiber Reinforced Self-Consolidating Concrete. *Constr. Build. Mater.* **2021**, *266*, 121102. [[CrossRef](#)]
60. Mastali, M.; Dalvand, A.; Sattarifard, A.R.; Abdollahnejad, Z.; Nematollahi, B.; Sanjayan, J.G.; Illikainen, M. A Comparison of the Effects of Pozzolan Binders on the Hardened-State Properties of High-Strength Cementitious Composites Reinforced with Waste Tire Fibers. *Compos. Part B Eng.* **2019**, *162*, 134–153. [[CrossRef](#)]
61. Zhang, S.; He, P.; Niu, L. Mechanical Properties and Permeability of Fiber-Reinforced Concrete with Recycled Aggregate Made from Waste Clay Brick. *J. Clean. Prod.* **2020**, *268*, 121690. [[CrossRef](#)]
62. Alsaif, A.; Bernal, S.A.; Guadagnini, M.; Pilakoutas, K. Durability of Steel Fibre Reinforced Rubberised Concrete Exposed to Chlorides. *Constr. Build. Mater.* **2018**, *188*, 130–142. [[CrossRef](#)]
63. Yazıcı, Ş.; İnan, G.; Tabak, V. Effect of Aspect Ratio and Volume Fraction of Steel Fiber on the Mechanical Properties of SFRC. *Constr. Build. Mater.* **2007**, *21*, 1250–1253. [[CrossRef](#)]
64. Afroughsabet, V.; Biolzi, L.; Ozbakkaloglu, T. High-Performance Fiber-Reinforced Concrete: A Review. *J. Mater. Sci.* **2016**, *51*, 6517–6551. [[CrossRef](#)]
65. Singh, N.; Singh, S.P. Carbonation and Electrical Resistance of Self Compacting Concrete Made with Recycled Concrete Aggregates and Metakaolin. *Constr. Build. Mater.* **2016**, *121*, 400–409. [[CrossRef](#)]
66. Nili, M.; Afroughsabet, V. The Long-Term Compressive Strength and Durability Properties of Silica Fume Fiber-Reinforced Concrete. *Mater. Sci. Eng. A* **2012**, *531*, 107–111. [[CrossRef](#)]
67. Kou, S.-C.; Poon, C.-S.; Etxeberria, M. Influence of Recycled Aggregates on Long Term Mechanical Properties and Pore Size Distribution of Concrete. *Cem. Concr. Compos.* **2011**, *33*, 286–291. [[CrossRef](#)]
68. Qureshi, L.A.; Ali, B.; Ali, A. Combined Effects of Supplementary Cementitious Materials (Silica Fume, GGBS, Fly Ash and Rice Husk Ash) and Steel Fiber on the Hardened Properties of Recycled Aggregate Concrete. *Constr. Build. Mater.* **2020**, *263*, 120636. [[CrossRef](#)]

Disclaimer/Publisher’s Note: The statements, opinions and data contained in all publications are solely those of the individual author(s) and contributor(s) and not of MDPI and/or the editor(s). MDPI and/or the editor(s) disclaim responsibility for any injury to people or property resulting from any ideas, methods, instructions or products referred to in the content.